Nonlinear Modal Analysis of Mechanical Systems with Frictionless Contact Interfaces

Denis Laxalde, Mathias Legrand

Nonlinear Modal Analysis of Mechanical Systems with Frictionless Contact Interfaces

Denis Laxalde*and Mathias Legrand
Structural Dynamics and Vibration Laboratory
Department of Mechanical Engineering
McGill University, Montreal, QC, Canada

Abstract

This paper explores mechanical systems undergoing unilateral frictionless contact conditions in the framework of nonlinear modal analysis. The nonlinear eigenproblem is formulated in the frequency domain through the minimization of a Rayleigh quotient subject to non-penetration inequality constraints. An additional equality constraint is introduced for normalization purposes. The resulting constrained minimization problem is then solved using an augmented Lagrangian strategy. Two applications are proposed: a thin longitudinal rod in unilateral contact with a rigid obstacle and a turbomachinery compressor blade in contact with a rigid casing. The first application illustrates the complexity of the nonlinear modal characterization of a system experiencing unilateral contact conditions while the second demonstrates the applicability of the proposed approach to large-scale mechanical systems involving non-smooth nonlinear terms.

Keywords: nonlinear modes; unilateral contact; Rayleigh quotient; Fourier methods; augmented Lagrangian; blades

1 Introduction

The concept of nonlinear mode is now commonly accepted as a reliable and well-suited approach for the analysis of nonlinear dynamical systems [1] since it offers the capability to extract the essential *signature* of nonlinear dynamical systems. While various analytical methods developed during the past decades have contributed to strengthen the relevant theoretical background, new challenges arise for large-scale mechanical systems [2]. As evidenced in the literature, promising techniques such as invariant manifold approaches [3], asymptotic-numerical methods [4], shooting techniques [5] or Fourier strategies [6] provide an appealing framework for the development of dedicated numerical tools which should bridge the gap between academic research and industrial applications.

Non-smooth nonlinearities such as unilateral contact yield other difficult challenges both on numerical and phenomenological sides that are not well tackled yet. Since unilateral contact is defined by a multi-valued evolution law which takes the form of inequality constraints, solution methods often fall in the theoretical field of optimization [7, 8] where the subsequent Lagrange multipliers play the role of the contact pressure field. Among other, augmented Lagrangian functionals stand as sophisticated and robust approaches to numerically approximate the latter, by transforming it into a smooth saddle point problem, and have been fruitfully applied in mechanical engineering [9, 10, 11].

In contact dynamics, numerical solution methods are mostly based on time integration and alternatives are unfortunately rarely explored [12, 13]. Accordingly, it seems challenging to regard this class of systems in the light of nonlinear modal analysis. In the present paper, the target application concerns rotating components in turbomachinery undergoing intermittent contacts (or impacts) with surrounding stationary

*Address all correspondence to this author.

structures. As a matter of fact, current design trends (more flexible and thinner structures) together with operating clearance reductions for aerodynamic efficiency purposes lead to complex and poorly known phenomena [14, 15, 16]. This, in particular, motivates the use of such modern techniques to extend existing design methodologies which currently mostly rely on linear analyses or time-stepping approaches.

The proposed approach is first described in the usual formalism of continuum mechanics. Eigensolutions are sought in the form of Fourier series which results in a mixed frequency-time boundary value problem. Then, introducing a variational formulation, the eigenvalue problem reduces to finding critical values of a generalized Rayleigh quotient functional in the admissible domain defined by the contact boundary conditions. This constrained minimization problem is then completed by an additional equality constraints which normalizes eigensolutions with reference with an energy. Finally, the resulting problem is solved in the framework of an augmented Lagrangian approach. Numerical approximations and algorithms are also detailed.

Two illustrative examples are investigated. The first considers a thin rod in unilateral contact with a rigid foundation and the second deals with a turbomachinery compressor blade in intermittent contact at its tip edge with a rigid casing. Consequences of unilateral contact on modal quantities are investigated.

2 Boundary value nonlinear eigenproblem

This section concerns the derivation of the strong nonlinear eigenvalue formulation of a flexible structure possibly in contact with a rigid foundation. Nonlinear modes [1] are defined as non-trivial periodic solutions of an autonomous dynamical system. Furthermore, in the present case, linear damping as well as friction are not considered so that the system is conservative.

2.1 Constitutive equations of the continuum

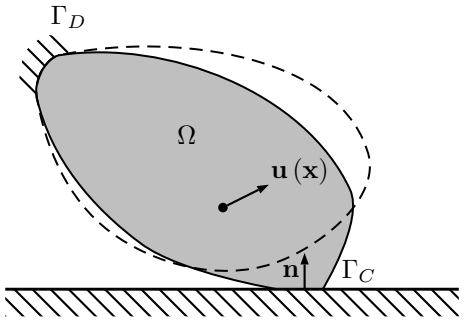

Figure 1: Notations

With reference to Fig. 1, we consider a flexible body occupying the open set Ω of $\mathbb{R}^d$ ($d = 2$ or 3) which boundary Γ consists of mutually disjoint open manifolds Γ_C (contact boundary), Γ_D (Dirichlet boundary) and Γ_F (Neumann boundary) such that $\bar{\Omega} = \Omega \cup \Gamma$. Since the system of interest is autonomous, the prescribed external forces are identically zero.

In the framework of infinitesimal deformations, the geometry of the current and reference configurations can not be distinguished. The displacement field of a material point $\mathbf{x}$ at time t is $\mathbf{u}(\mathbf{x}, t)$. The linearized strain tensor mapping displacements to deformations is expressed as $\varepsilon = \frac{1}{2}\left(\nabla\mathbf{u} + \nabla^T\mathbf{u}\right)$ and the linearized stress tensor as $\sigma = \mathcal{A} : \varepsilon$, in which $\mathcal{A}$ denotes the fourth-order elasticity tensor associated with the constitutive symmetric and hyper-elastic linear Hooke's law, allowing for the formulation of a differentiable stored strain energy. For any material point $\mathbf{x}$ belonging to contact boundary Γ_C, we uniquely define, for each $\mathbf{x} \in \Gamma_C$, a gap function

$$g(\mathbf{u}) = \mathbf{u}(\mathbf{x}, t) \cdot \mathbf{n} - g_0(\mathbf{x}) \tag{1}$$

linear with respect to the displacement field $\mathbf{u}$, and the contact pressure

$$\tau_N = \sigma \cdot \mathbf{n} \tag{2}$$

where $\mathbf{n}$ stands as the outward normal vector (independent of the displacement field in an infinitesimal deformations framework) and $g_0(\mathbf{x})$ is the initial positive gap.

Accordingly, the boundary value problem, describing the motion of the continuum structure parameterized in space and time, may be written as

$$\rho\ddot{\mathbf{u}} - \operatorname{div}\boldsymbol{\sigma}(\mathbf{u}) = 0 \quad \text{on} \quad \Omega \times \mathbb{R}_*^+ \tag{3a}$$

$$\mathbf{u} = 0 \quad \text{on} \quad \Gamma_D \times \mathbb{R}_*^+ \tag{3b}$$

$$g(\mathbf{u}) \leq 0, \quad \tau_N \geq 0, \quad g(\mathbf{u}) \cdot \tau_N = 0 \quad \text{on} \quad \Gamma_C \times \mathbb{R}_*^+ \tag{3c}$$

Eq. (3a) describes the local dynamic equilibrium, Eq. (3b) is the Dirichlet boundary condition and Eq. (3c) defines the Signorini boundary conditions, implying impenetrability, compression and complementary conditions [17]. These constraints preclude any possible inter penetration between the mechanical bodies in presence. We adopt the convention that the "gap" is negative for admissible (i.e. non-penetrated) deformations. Also note that the usual initial conditions are omitted here since they are not relevant for the particular class of periodic solutions of interest.

In the sequel, the derivation of the nonlinear eigenvalue problem is introduced. As eigensolutions are sought in the form of Fourier series, problem (3) will be transformed into a so-called mixed frequency-time eigenvalue problem.

2.2 Mixed frequency-time eigenvalue problem

Since we are interested in non-trivial periodic solutions to problem (3), it seems natural to expand the displacement field in the frequency domain using Fourier series:

$$\mathbf{u}(t) = \sum_{n\in\mathbb{Z}} \hat{\mathbf{u}}_n e^{\mathrm{j}n\omega t} \quad \text{with} \quad \hat{\mathbf{u}}_n = \frac{1}{T}\int_T \mathbf{u}(t) e^{-\mathrm{j}n\omega t}\,\mathrm{d}t \tag{4}$$

in which $\omega = 2\pi/T$ is the fundamental nonlinear eigenfrequency of the motion to be determined.

The eigenvalue problem consists in finding $\{\omega, \hat{\mathbf{u}}\}$, with $\hat{\mathbf{u}} = \{\hat{\mathbf{u}}_n,\ n \in \mathbb{Z}\}$ such as,

$$-\operatorname{div}\boldsymbol{\sigma}(\hat{\mathbf{u}}_n) = (n\omega)^2 \rho \hat{\mathbf{u}}_n \quad \text{on} \quad \Omega \times \mathbb{Z} \tag{5a}$$

$$\hat{\mathbf{u}}_n = 0 \quad \text{on} \quad \Gamma_D \times \mathbb{Z} \tag{5b}$$

$$g(\hat{\mathbf{u}}) \leq 0, \quad \tau_N \geq 0, \quad g(\hat{\mathbf{u}}) \cdot \tau_N = 0 \quad \text{on} \quad \Gamma_C \times [0, T] \tag{5c}$$

in which the gap function is now expressed using Eq. (4) as:

$$g(\hat{\mathbf{u}}) = \sum_{n\in\mathbb{Z}} \hat{\mathbf{u}}_n \cdot \mathbf{n}\ e^{\mathrm{j}n\omega t} - g_0 \tag{6}$$

Note that while Eqs. (5a) and (5b) are formulated in the frequency domain, Eq. (5c) requires the use of time, by definition. Accordingly, (5) is called a mixed frequency-time domains boundary value problem.

Even though the introduced strong formulation is not of much help for the characterization of a possible solution, it brings light to the intrinsic complexity of the inherent hybrid time-frequency properties of the system due to the direct relationships between the contact tractions subject to spatial geometric constraints themselves dependent on the unknown deformation mappings.

3 Variational formulation

Strong formulations such as the one detailed above suffer too restrictive assumptions on the class of functions which the solution is sought into. Most of the classical and intuitive conditions of smoothness are not suitable for proving the existence and uniqueness of a solution. Instead, an integral counterpart of system (5) can be derived within the proper mathematical framework of variational formulations.

3.1 Constrained minimization of Rayleigh quotient

In this section, the variational formulation associated with the nonlinear eigenproblem defined by Eqs. (5) is derived using the concept of Rayleigh quotient minimization. As a preamble, let us define the following space of admissible displacements

$$\mathcal{V}_g = \{\mathbf{u} \in \mathcal{V},\ g(\mathbf{u}) \leq 0 \text{ on } \Gamma_C\} \tag{7}$$

which accounts for Signorini boundary conditions and is a closed convex subset of the Sobolev space

$$\mathcal{V} = \{\mathbf{u} : \bar{\Omega} \to \mathbb{R}^d \text{ such as } \mathbf{u} \in (\mathbf{H}^1(\Omega))^d \text{ and } \mathbf{u}|_{\Gamma_D} = 0\} \tag{8}$$

equipped with the classical scalar product $\langle \cdot, \cdot \rangle$ and norm $\|\cdot\|$.

Let us also define the usual bilinear and symmetric potential and kinematic energy functionals on $\mathcal{V}\times\mathcal{V}$ to characterize the modal displacements of the system:

$$\mathrm{m}(\mathbf{u}, \mathbf{v}) = \int_\Omega \rho \mathbf{u}\mathbf{v}\, \mathrm{d}\mathbf{x} \tag{9a}$$

$$\mathrm{k}(\mathbf{u}, \mathbf{v}) = \int_\Omega \boldsymbol{\sigma}(\mathbf{u}) : \boldsymbol{\epsilon}(\mathbf{v})\ \mathrm{d}\mathbf{x} \tag{9b}$$

The following generalized Rayleigh quotient can then be built:

$$\mathrm{r}(\hat{\mathbf{u}}) = \frac{\hat{\mathrm{k}}(\hat{\mathbf{u}}, \hat{\mathbf{u}})}{\hat{\mathrm{m}}(\hat{\mathbf{u}}, \hat{\mathbf{u}})} \tag{10}$$

in which the two frequency-domain energy functionals follow from Eqs. (9) as

$$\hat{\mathrm{k}}(\hat{\mathbf{u}}, \hat{\mathbf{u}}) = \sum_{n\in\mathbb{Z}} \mathrm{k}(\hat{\mathbf{u}}_n, \hat{\mathbf{u}}_n) \quad \text{and} \quad \hat{\mathrm{m}}(\hat{\mathbf{u}}, \hat{\mathbf{u}}) = \sum_{n\in\mathbb{Z}} n^2\, \mathrm{m}(\hat{\mathbf{u}}_n, \hat{\mathbf{u}}_n) \tag{11}$$

Nonlinear eigenvectors $\hat{\mathbf{u}}$ are defined as critical points of this Rayleigh quotient and the associated eigenvalues are such that $\omega^2 = \mathrm{r}(\hat{\mathbf{u}})$. Due to Signorini conditions, which confine the space of admissible displacements to (7), this minimization problem is constrained. Furthermore, eigensolutions should be normalized. This is even more important in a nonlinear framework due to the energy dependency of the modal parameters. An usual approach (which also brings physical sense) is to normalize eigenvectors with respect to the kinetic energy (often called mass normalization). We hence define the following functional

$$h(\hat{\mathbf{u}}) = \frac{1}{2}\hat{\mathrm{m}}(\hat{\mathbf{u}}, \hat{\mathbf{u}}) - \gamma \tag{12}$$

which relates the kinetic energy to the modal coordinate γ.

Accordingly, the eigenproblem of interest becomes

$$\min_{\hat{\mathbf{u}}_n \in \mathcal{V}_g} \mathrm{r}(\hat{\mathbf{u}}) \text{ subject to } h(\hat{\mathbf{u}}) = 0 \tag{13}$$

3.2 Lagrangian formulation

Consider now the following Lagrangian

$$\mathcal{L}(\hat{\mathbf{u}}, \lambda, \mu) = \mathrm{r}(\hat{\mathbf{u}}) + \int_T \langle \lambda(t), g(\hat{\mathbf{u}}) \rangle\, \mathrm{d}t + \mu h(\hat{\mathbf{u}}) \tag{14}$$

in which $\lambda(t)$ is a time-dependent and positive Lagrange multiplier field and μ is a (constant) Lagrange multiplier. The initial constrained minimization problem (13) can be converted into a saddle point problem:

$$\min_{\hat{\mathbf{u}}_n \in \mathcal{V}} \max_{\lambda > 0} \mathcal{L}(\hat{\mathbf{u}}, \lambda, \mu) \tag{15}$$

This Lagrangian formulation enables the use of unrestricted displacement spaces $\mathcal{V}$ by transferring the constraints to the Lagrange multiplier dual variables. As a consequence, optimality conditions associated with problem (15) are

$$\nabla_{\hat{\mathbf{u}}_n} \mathrm{r}(\hat{\mathbf{u}}) + \int_T \langle \lambda(t), \nabla_{\hat{\mathbf{u}}_n} g(\hat{\mathbf{u}}) \rangle \, \mathrm{d}t + \mu \nabla_{\hat{\mathbf{u}}_n} h(\hat{\mathbf{u}}) = 0 \quad \forall n \in \mathbb{Z} \tag{16a}$$

$$g(\hat{\mathbf{u}}) \leq 0, \;\; \lambda(t) > 0 \;\; \text{and} \;\; \langle \lambda(t), g(\hat{\mathbf{u}}) \rangle = 0 \quad \forall t \in [0, T] \tag{16b}$$

$$h(\hat{\mathbf{u}}) = 0 \tag{16c}$$

They can be expanded, yielding the following variational formulation:

Find $\{\hat{\mathbf{u}}_n \in \mathcal{V}, \; n \in \mathbb{Z}\}$ *such as* $\forall \mathbf{v} \in \mathcal{V}$

$$\begin{aligned} &2\,\mathrm{m}\left(\hat{\mathbf{u}}_n, \hat{\mathbf{u}}_n\right)^{-1} \left(\mathrm{k}\left(\hat{\mathbf{u}}_n, \mathbf{v}\right) - n^2\,\mathrm{r}\left(\hat{\mathbf{u}}\right)\mathrm{m}\left(\hat{\mathbf{u}}_n, \mathbf{v}\right)\right) \\ &\qquad + \int_T \langle \boldsymbol{\lambda}, \mathbf{v} \rangle e^{\mathrm{j}n\omega t} \, \mathrm{d}t + 2\mu\,\mathrm{m}\left(\hat{\mathbf{u}}_n, \mathbf{v}\right) = 0 \quad \forall n \in \mathbb{Z} \end{aligned} \tag{17a}$$

$$g(\hat{\mathbf{u}}) \leq 0, \;\; \boldsymbol{\lambda} > 0 \;\; \text{and} \;\; \langle \boldsymbol{\lambda}, g\left(\hat{\mathbf{u}}\right) \rangle = 0 \quad \forall t \in [0, T] \tag{17b}$$

$$h(\hat{\mathbf{u}}) = 0 \tag{17c}$$

Similarly to linear systems, solutions of system (17) are critical points of constrained Rayleigh quotient (13). Under general yet conservative assumptions, one would have to account for the contribution of nonlinear internal forces in the potential energy of the system and then consider the minimization of the subsequently modified Rayleigh quotient. In the present study, since nonlinear forces arise from contact boundary conditions, their work is identically zero; hence the use of an unmodified Rayleigh quotient to define the respective eigenvalues.

3.3 Augmented Lagrangian

The saddle point formulation (15) and the subsequent derivations, equivalent to the original nonlinear eigenvalue problem (13), are formulated in the augmented Lagrangian framework. As a matter of fact, this formulation improves convergence and computationally benefits from the addition of penalty terms on constraints, allowing for the implementation of efficient Uzawa-like solution algorithms that perform descent on the primal displacement variable, through traditional nonlinear solvers, and ascent on the dual Lagrange multipliers (coinciding with contact forces when convergence is reached).

Among all the alternatives, the augmented Lagrangian is here defined as [18]:

$$\mathcal{L}_\kappa\left(\hat{\mathbf{u}}, \theta\right) = \mathrm{r}\left(\hat{\mathbf{u}}\right) + \frac{1}{2}\int_T \left\| \sqrt{\kappa_i}\left(g\left(\hat{\mathbf{u}}\right) + \theta_i\right)\right\|_+^2 \mathrm{d}t + \frac{1}{2}\kappa_e\left(h(\hat{\mathbf{u}}) + \theta_e\right)^2 \tag{18}$$

in which $\kappa_i\theta_i$ and $\kappa_e\theta_e$ represent Lagrange multipliers for inequality and equality constraints respectively. The diagonal matrix κ_i and scalar κ_e are respective positive penalty parameters. By first defining the dual parameters $\theta = \{\theta_i, \theta_e\}$ and $\kappa = \{\kappa_i, \kappa_e\}$, the principle of such strategies is to generate a sequence of primal iterates $\hat{\mathbf{u}}^{(j)}$, which minimize the augmented Lagrangian (18) for constant multipliers $\theta^{(j)}, \kappa^{(j)}$ which are subsequently updated, in agreement with the constraints.

The optimality condition for the minimization of the augmented Lagrangian functional (18) is:

$$\nabla_{\hat{\mathbf{u}}_n} \mathcal{L}_\kappa\left(\hat{\mathbf{u}}, \theta\right) = 0 \quad \forall n \in \mathbb{Z} \tag{19}$$

which, according to Eqs. (17), may be written as:

Find $\{\hat{\mathbf{u}}_n \in \mathcal{V},\ n \in \mathbb{Z}\}$ *such as* $\forall \mathbf{v} \in \mathcal{V}$

$$2\,\mathrm{m}\left(\hat{\mathbf{u}}_n, \hat{\mathbf{u}}_n\right)^{-1}\left(\mathrm{k}\left(\hat{\mathbf{u}}_n, \mathbf{v}\right) - n^2\omega^2\left(\hat{\mathbf{u}}\right)\mathrm{m}\left(\hat{\mathbf{u}}_n, \mathbf{v}\right)\right) + \int_T \langle \kappa_i \left(g\left(\hat{\mathbf{u}}\right) + \boldsymbol{\theta}_i\right)_+, \mathbf{v}\rangle e^{\mathrm{j}n\omega t}\,\mathrm{d}t + \kappa_e\,\mathrm{m}\left(\hat{\mathbf{u}}_n, \mathbf{v}\right)\left(h\left(\hat{\mathbf{u}}\right) + \theta_e\right) = 0 \quad (20)$$

where parameter θ is then adjusted as follows:

$$\theta_i \leftarrow \theta_i + \max_{\mathbf{x},t}\left(g\left(\hat{\mathbf{u}}\right), -\theta_i\right) \quad (21a)$$

$$\theta_e \leftarrow \theta_e + h(\hat{\mathbf{u}}) \quad (21b)$$

The penalty coefficients κ may also be updated when conditions (21) did not improve the constraints.

4 Numerical implementation and algorithm

In the framework of finite-element method, we consider a discretized displacement field $\mathbf{U}$ together with consistent mass $\mathbf{M}$ and stiffness $\mathbf{K}$ structural matrices based on (9). Furthermore, a uniform time discretization is introduced:

$$t = \{t_k = kT/m,\ k = 1, \ldots, m\} \quad (22)$$

such as $\bar{\mathbf{U}}_k = \mathbf{U}\left(t_k\right)$ are discrete time values of $\mathbf{U}$ and the Fourier series of Eq. (4) is truncated up to order N. Hence, frequency-domain and time-domain variables are now related to each other in a discrete form:

$$\hat{\mathbf{U}}_n = \frac{1}{T}\sum_{k=1}^{m} \bar{\mathbf{U}}_k e^{-\mathrm{j}\frac{2\pi kn}{m}} \quad \text{and} \quad \bar{\mathbf{U}}_k = \sum_{n=-N}^{N} \hat{\mathbf{U}}_n e^{\,\mathrm{j}\frac{2\pi kn}{m}} \quad (23)$$

In practical applications, it is usually required to have N significantly smaller than m.

Within these numerical assumptions, the mixed frequency-time augmented Lagrangian eigenvalue problem consists of:

- the discretized Rayleigh quotient, used to calculate eigenvalues

$$\mathrm{r}(\hat{\mathbf{U}}) = \frac{\displaystyle\sum_{n=-N}^{N} \hat{\mathbf{U}}_n^* \mathbf{K} \hat{\mathbf{U}}_n}{\displaystyle\sum_{n=-N}^{N} n^2 \hat{\mathbf{U}}_n^* \mathbf{M} \hat{\mathbf{U}}_n} \quad (24a)$$

- the gap function (6) as a linear system of equations for each time-step k:

$$\left\{\mathbf{g}(\bar{\mathbf{U}}_k) = \mathbf{A}\bar{\mathbf{U}}_k - \mathbf{g}_0,\ 1 \le k \le m\right\} \quad (24b)$$

  where rectangular matrix $\mathbf{A}$ restricts the displacement vector $\mathbf{U}$ to contact degrees-of-freedom;

- the mode normalization (12):

$$h(\hat{\mathbf{U}}) = \frac{1}{2}\sum_{n=-N}^{N} \hat{\mathbf{U}}_n^* \mathbf{M} \hat{\mathbf{U}}_n - \gamma \quad (24c)$$

- the eigenvalue equation (20) which reduces to $2N+1$ coupled sub-problems:

$$2\mathbf{M}^{-1}\left(\mathbf{K} - (n\omega)^2\mathbf{M}\right)\hat{\mathbf{U}}_n + \mathbf{A}^T \sum_{k=1}^{m} \kappa_i \big(\mathbf{g}(\bar{\mathbf{U}}_k) + \theta_{i,k}\big)_+ e^{\mathrm{j}\frac{2\pi kn}{m}} + \kappa_e \big(h(\hat{\mathbf{U}}) + \theta_e\big)\mathbf{M}\hat{\mathbf{U}}_n = 0 \quad (24d)$$

Algorithm 1 Nonlinear modal analysis: simultaneous eigenfrequency/eigenvector resolution

Set $j = 0$, $\{\omega^{(0,p)},\ \hat{U}^{(0,p)}\}$
for $h^{(j)}$ in $[h_{min} \dots h_{max}]$ **do**
    Solve the augmented Lagrangian problem (Eqs. (24d) and (24b)-(24c)) and the Rayleigh quotient Eq. (24a) for $\{\omega^{(j)},\ \hat{U}^{(j)}$ using Algorithm 3
    Predict $\{\omega^{(j+1,p)},\ \hat{U}^{(j+1,p)}\}$
end for

Algorithm 2 Nonlinear modal analysis: sequential eigenfrequency/eigenvector resolution

Set $j = 0$, $\{\omega^{(0,p)},\ \hat{U}^{(0,p)}\}$
for $h^{(j)}$ in $[h_{min} \dots h_{max}]$ **do**
    Solve the augmented Lagrangian problem (Eqs. (24d) and (24b)-(24c)) for $\hat{U}^{(j)}$ with $\omega = \omega^{(j,p)}$ using Algorithm 3
    Retrieve eigenvalue $\omega^{(j)}(\hat{U}^{(j)})$ using the Rayleigh quotient, Eq. (24a)
    Predict $\{\omega^{(j+1,p)},\ \hat{U}^{(j+1,p)}\}$
end for

Various techniques can be employed to solve the eigenvalue problem defined by Eqs. (24). In particular, we have considered a combined and a sequential approach in which the eigenvalue and eigenvector are found either simultaneously or sequentially as described by Algorithms 1 and 2 respectively. The simultaneous approach is more rigorous yet computationally more expensive (in particular concerning the calculations and updates of Hessians). The sequential approach requires the energy-steps ($\delta h^{(i)}$) to be sufficiently small to ensure that an approximate eigenvalue does not significantly affect the accuracy of the resulting eigenvector. Provided the latter condition is satisfied, the simultaneous and sequential approaches would yield similar results. In both approaches, Eq. (24d) is numerically solved using a dedicated augmented Lagrangian algorithm, inspired by the one detailed in [19]. The proposed algorithm 3 offers the following features:

- Convergence is controlled using Powell's measures of convergence:

$$G_i = \max_{\text{dof}} |\max_k \left(\mathbf{g}\left(\bar{\mathbf{U}}_k\right), -\theta_{i,k}\right)| \tag{25a}$$

$$G_e = |h(\hat{\mathbf{U}})| \tag{25b}$$

- Updates of multipliers and penalty parameters are determined depending on whether constraints have sufficiently improved, that is to say, for each constraint which does not satisfy:

$$\max\left(\mathbf{g}(\bar{\mathbf{U}}_k), \theta_{i,k}\right) < \frac{G_i}{\alpha} \tag{26a}$$

$$h(\hat{\mathbf{U}}) < \frac{G_e}{\alpha} \tag{26b}$$

The numerical implementation is performed in Python programming language with the help of NumPy/SciPy [20] scientific libraries.

5 Applications

This section concerns two applications which illustrate the proposed methodology and algorithms. The first is dedicated to the study a thin rod in contact with a rigid obstacle at one of its boundary and the second focuses on a turbomachinery compressor blade in contact with a rigid contact interface at its tip edge.

Algorithm 3 Augmented Lagrangian with equality and inequality constraints

Set $j = 0$, $j_{\max}$, $G_{i,e}^{(0)} = \infty$, $\theta = \theta^{(1)}$, $\kappa = \kappa^{(1)}$
Choose $\alpha > 1$, $\beta > 1$, $\epsilon > 0$
while $j < j_{\max}$ **do**
  Solve Eq. (24d) for $\{\hat{\mathbf{U}}_n\}_{n=-N,\dots,N}$ with fixed or variable ω (according to Algorithms 1 or 2)
  Evaluate constraints $\{\mathbf{g}(\bar{\mathbf{U}}_k)\}_{k=1,\dots,m}$ and $h(\hat{\mathbf{U}})$ using Eqs. (24b) and (24c)
  Set Powell's criteria $\bar{G}_i$ and $\bar{G}_e$ according to Eqs. (25)
  if $\bar{G}_i < \epsilon$ and $\bar{G}_e < \epsilon$ **then**
    break
  else
    $j \leftarrow j + 1$
    if $\bar{G}_i \geq \epsilon$ **then** ▷ *Inequality constraints*
      Set $\mathbf{S}_i = \{l : |\max\left(\mathbf{g}(\bar{\mathbf{U}}_k), -\theta_{i,k}\right)| \geq G_i^{(j)}/\alpha\}$ ▷ Constraints to be improved, Eq. (26a)
      if $\bar{G}_i \geq G_i^{(j)}$ **then** ▷ Increase penalty parameters selectively
        $\forall l \in \mathbf{S}_i$, $\kappa_{i,l} \leftarrow \beta\kappa_{i,l}$ and $\theta_{i,l} \leftarrow \theta_{i,l}/\beta$
      else ▷ Update multipliers
        $\theta_i^{(j)} \leftarrow \theta_i$, $\kappa_i^{(j)} \leftarrow \kappa_i$ and $G_i^{(j)} \leftarrow \bar{G}_i$
        $\theta_i \leftarrow \theta_i^{(j)} + \max_k\left(\mathbf{g}(\bar{\mathbf{U}}), -\theta_i\right)$
        if $G_i^{(j)} \geq G_i^{(j-1)}/\alpha$ **then** ▷ Inequality constraints did not improve enough
          $\forall l \in \mathbf{L}_i$, $\kappa_{i,l} \leftarrow \beta\kappa_{i,l}$ ▷ Increase penalty parameters selectively
        end if
      end if
    end if
    if $\bar{G}_e \geq \epsilon$ **then** ▷ *Equality constraints*
      if $\bar{G}_e \geq G_e^{(j)}$ **then** ▷ Test Eq. (26b)
        $\kappa_e \leftarrow \beta\kappa_e$ and $\theta_e \leftarrow \theta_e/\beta$ **if** $h(\hat{\mathbf{U}}) < G_e/\alpha$ ▷ Increase penalty parameter
      else ▷ Update multiplier
        $\theta_e^{(j)} \leftarrow \theta_e$, $\kappa_e^{(j)} \leftarrow \kappa_e$ and $G_e^{(j)} \leftarrow \bar{G}_e$
        $\theta_e \leftarrow \theta_e^{(j)} + h_\gamma(\hat{\mathbf{U}})$
        if $G_e^{(j)} \geq G_e^{(j-1)}/\alpha$ **then** ▷ Equality constraints did not improve enough
          $\kappa_e \leftarrow \beta\kappa_e$ **if** $|h(\hat{\mathbf{U}})| \geq G_e/\alpha$ ▷ Increase penalty parameter
        end if
      end if
    end if
  end if
end while

5.1 Thin rod in contact against a rigid foundation

We first investigate the first nonlinear mode of a simple rod undergoing hybrid force-displacement unilateral constraints, as depicted in Fig. 2. The natural frequency of its linear counterpart with clamped-free boundary

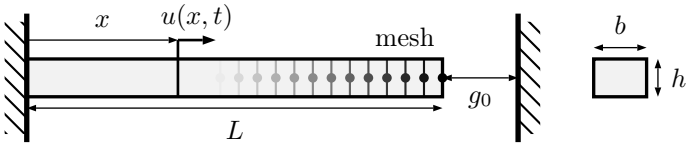

Figure 2: Thin rod in contact against a rigid foundation

conditions is 1297.5 Hz. The initial gap g_0 is used for the normalization of all subsequent results. Since the system is assumed to be hyper-elastic, results are not sensitive to the initial gap amplitude. The mechanical characteristics of the rod are as follows: $E = 2.1 \times 10^{11}$ Pa (Young modulus), $\rho = 7800$ kg/m^3 (mass per unit volume), $L = 1$ m (length) and $A = h \times b = 0.03 \times 0.03$ m^2 (cross section area).

The equations of motion can be summarized as:

- local equation:

$$\rho \frac{\partial^2 u}{\partial t^2}(x,t) - E \frac{\partial^2 u}{\partial x^2}(x,t) = 0, \quad x \in]0, L[\tag{27a}$$

- boundary condition:

$$u(0,t) = 0 \tag{27b}$$

- unilateral contact conditions:

$$u(L,t) - g_0 \leq 0, \quad \sigma_{xx}(L,t) = EA \frac{\partial u}{\partial x}(L,t) \geq 0, \quad (u(L,t) - g_0) \cdot \sigma_{xx}(L,t) = 0 \tag{27c}$$

The numerical nonlinear modal analysis is conducted with a separate solution $u(x,t) = \mathbf{N}(x)^T \mathbf{h}(t)$ constructed through the usual finite element discretization involving $n = 20$ rod elements and the following respective elementary mass and stiffness matrices:

$$M_e = \frac{\rho A \ell_e}{6} \begin{bmatrix} 2 & 1 \\ 1 & 2 \end{bmatrix} \quad \text{and} \quad K_e = \frac{EA}{\ell_e} \begin{bmatrix} 1 & -1 \\ -1 & 1 \end{bmatrix}, \quad \ell_e = \frac{L}{n} \tag{28}$$

After space-integration over the length of the rod, the unknown modal displacement field is given by Eq. (4) and the eigenvalue problem derived from Eqs. (27) is solved with Algorithm 2. As already explained, the mode normalization of Eq. (24c) through a prescribed kinetic energy controls the amplitude of the nonlinear mode.

Fig. 3 displays the first nonlinear mode eigenfrequency with respect to the modal energy (normalized with reference with the initial gap). Contact occurs as soon as the modal energy reaches unity. Then, the natural frequency increases which denotes a hardening effect. Figs. 4 display a portion of the nonlinear internal distribution of the rod nodal displacements over a motion period, namely the displacements of the first and last nodes versus the displacement and velocity of the middle node of the rod. Again, differences between linear and nonlinear regimes are noticeable. While the former typically features elliptic trajectories in the phase space, the latter is much more complex with velocity singularities and quick changes in displacements.

Further details about this complex motion can be extracted from Figs. 5, which depict time-histories of all degrees-of-freedom for two normalized modal energies, respectively 0.7 (without contact) and 1.8 (with contact). When the prescribed kinetic energy is low, the usual first mode of the rod is retrieved as pictured in Fig. 5(a)-(b). In this configuration, the mode is a standing wave for which displacement and velocity fields are algebraically related through a phase-shift and an amplitude ratio, as expected. Maximum displacement and

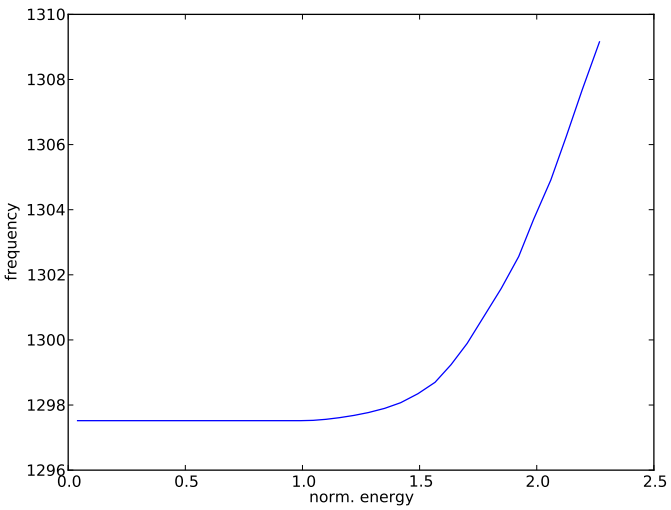

Figure 3: Frequency-energy plot of the first nonlinear mode

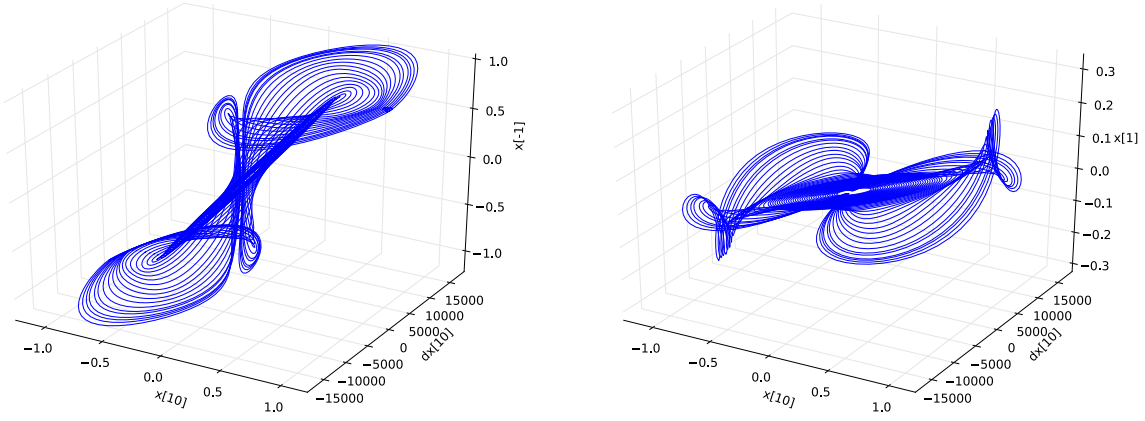

(a) (b)

Figure 4: Periodic motions of the first nonlinear mode represented in a three-dimensional projection of the phase space; Displacements of the (a) last and (a) first nodes versus displacement and velocity of the middle node.

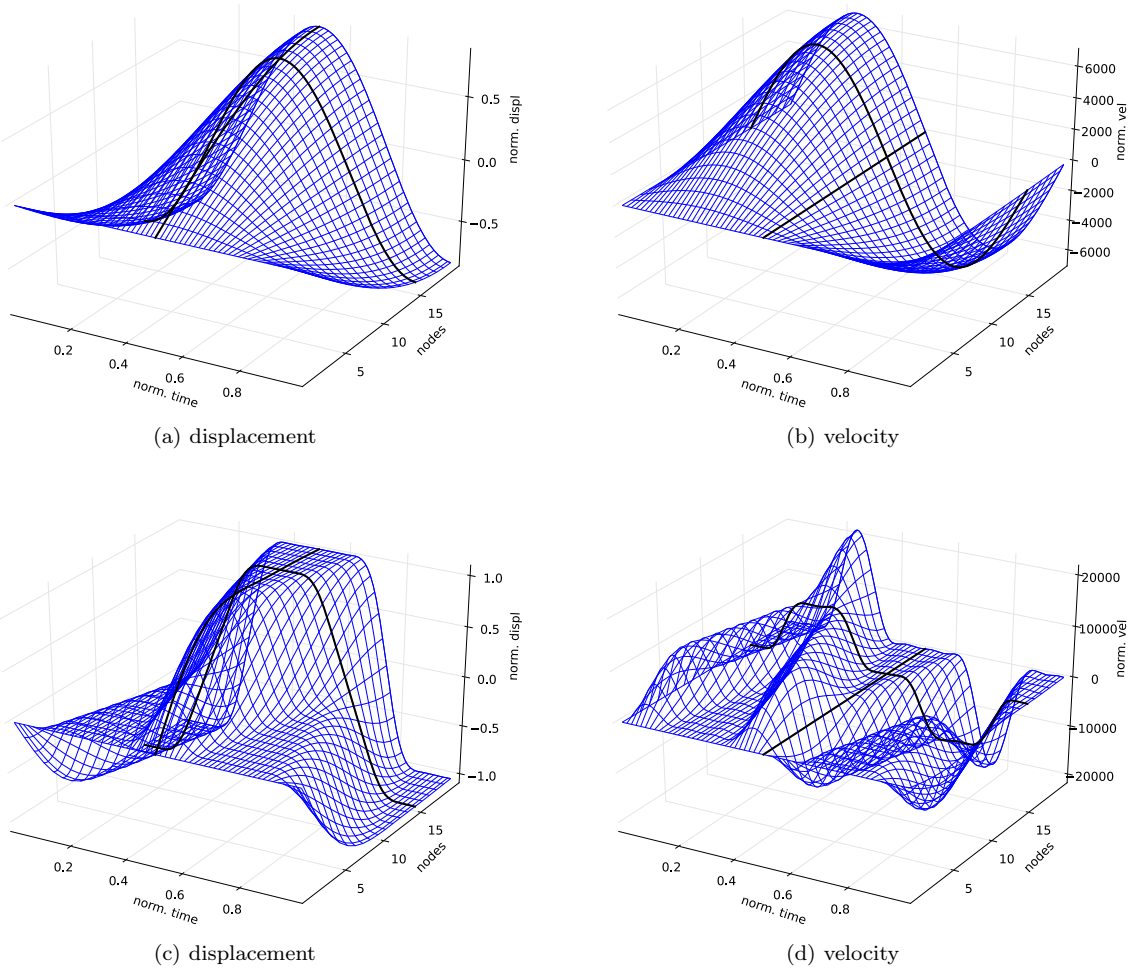

(a) displacement

(b) velocity

(c) displacement

(d) velocity

Figure 5: Time-histories of rod's displacement and velocity degrees-of-freedom for normalized energy 0.7 ((a) and (b)) and 1.8 ((c) and (d))

(respectively) velocity nodal amplitudes are simultaneously reached. On the contrary, when the prescribed kinetic energy is such that the tip of the rod hits the rigid foundation (normalized energy = 1.8), contact occurs over a fraction of the period of the respective nonlinear mode which becomes a traveling wave, as displayed in Fig. 5(c)-(d). Displacement and velocity fields are no more algebraically related to each other. As a matter of fact, under proper assumptions, Eq. (27a) generically admits a combination of forward and backward travelling wave solutions: these are highlighted by the velocity map histories in Fig. 5d for which the condition of simultaneous maximum nodal amplitudes does not hold anymore. Furthermore, the expected symmetry in time and space of generic travelling waves is also retrieved by the algorithm as pictured in Fig. 5c while no assumptions were made on the displacement field.

5.2 A turbomachinery blade in contact at its tip edge

The second application concerns a turbomachinery compressor blade in contact with a rigid contact interface at its tip edge. This situation is representative of rotating compressor components experiencing unilateral contacts with surrounding rigid casings. The finite element model of this blade is shown in Fig. 6 where the red nodes define the contact interface. This model is reduced by means of a Craig-Bampton procedure

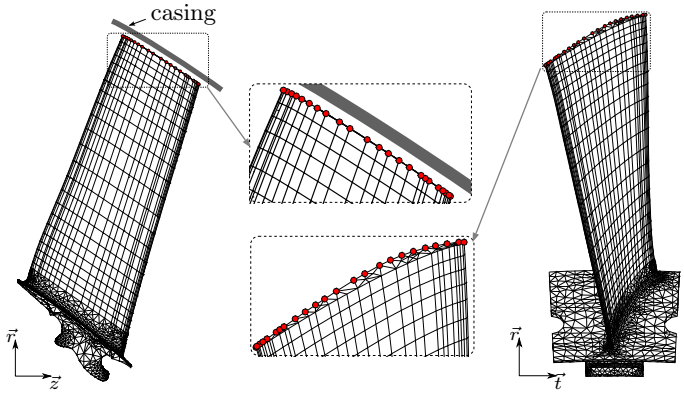

Figure 6: Blade model and details of the contact interface

composed of 72 constraints modes associated with the physical displacements of 24 retained interface nodes belonging to the contact surface Γ_C complemented by 40 component normal modes. Contact occurs in the radial direction only and a uniform initial gap is assumed. All displacements and velocities are normalized with respect to this initial gap and nonlinear frequencies are normalized with respect to the first linear frequency of the blade.

Fig. 7 depicts the eigenfrequency of the first mode (nonlinear extension of the first bending mode of the blade) with respect to the modal energy. When the normalized energy is greater that one, intermittent contacts occur at the leading and trailing edges of the contact interface. This results in an increase of the natural frequency of the blade.

Figs. 8 display the mode shapes for three values of the modal energy. Sensitivity of mode shapes to contacts is noticeable. In particular, torsion effects tends to appear as modal energy increases and contact becomes more prominent.

This example illustrates a potential application of nonlinear modal analysis in an engineering perspective. Indeed, modal characteristics provide a straightforward on assessment of the effects of contacts on blades' dynamics (change of frequencies, stress concentrations, etc.) One can then image the development of design tools based on nonlinear modal analysis such as nonlinear Campbell diagrams.

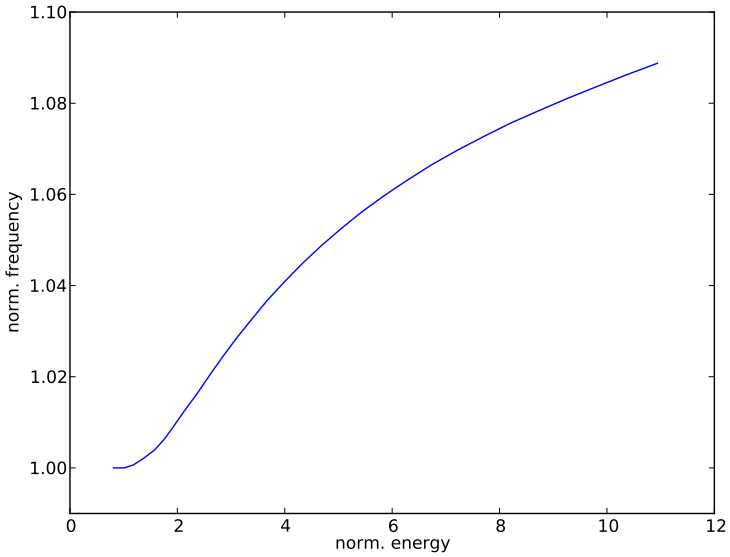

Figure 7: Frequency / energy plot of the first nonlinear mode of the blade

6 Conclusions

A methodology for the modal analysis of elastic structures with contact interfaces is proposed. Based on the definition of nonlinear modes as non-trivial periodic solutions of the autonomous dynamical system, the eigenvalue problem is defined in a continuum framework and involves Signorini boundary conditions. A generalized Rayleigh quotient functional is introduced, which minimization under constraints is formulated using Lagrange multipliers, and solved using an augmented Lagrangian technique. Numerical approximations in space, time and frequency are then proposed for the sake of numerical treatments.

The approach is first illustrated on the example of thin rob in contact at one of its end. Interesting travelling wave motions for a conservative nonlinear system are obtained. Then, a turbomachinery compressor blade in contact with a rigid casing is considered. The first nonlinear mode is studied using the developed numerical tool and the sensitivity of the modal quantities to the contact constraints is explored. Stability and bifurcations analyses of motions of interest may be provided in future research works. Friction effects as well as wear along the contact interfaces can also be implemented.

Nonlinear modal analysis may have long-term applications in the characterization of time-stepping techniques by measuring their capabilities to remain on the respective nonlinear manifolds.

Acknowledgment

Thanks go to Snecma for its technical and financial support. This work takes place in the framework of the MAIA mechanical research and technology program sponsored by CNRS, ONERA and SAFRAN Group.

References

[1] A. F. Vakakis, L. I. Manevitch, Y. V. Mikhlin, V. N. Pilipchuk, and A. A. Zevin. *Normal Modes and Localization in Nonlinear Systems*. Wiley series in nonlinear science, 1996. doi:10.1002/9783527617869.

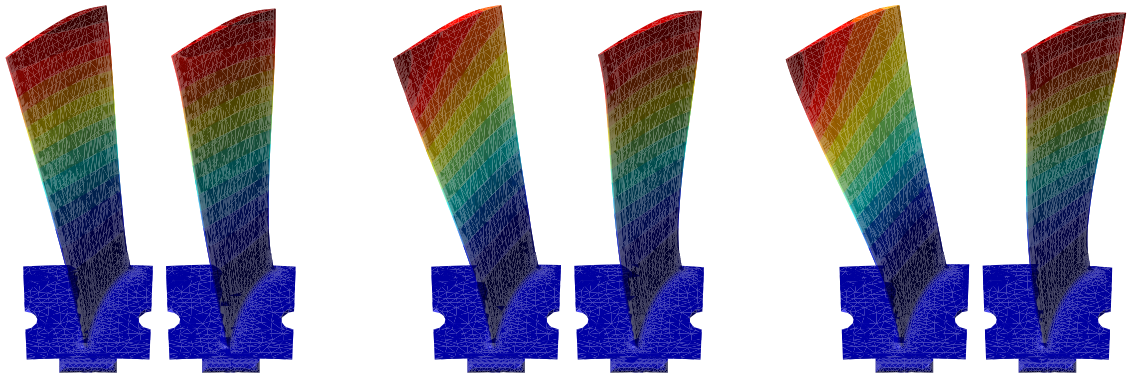

(a) (b) (c)

Figure 8: Mode shapes for three modal amplitudes: (a) 0.8, (b) 4.7 and (c) 10.4 and at $t = 0$ and $t = T/2$.

[2] G. Kerschen, M. Peeters, J. Golinval, and A. Vakakis. Nonlinear normal modes, part I: A useful framework for the structural dynamicist. *Mechanical Systems and Signal Processing*, 23(1):170, 2009. doi:10.1016/j.ymssp.2008.04.002.

[3] E. Pesheck, C. Pierre, and S. W. Shaw. A new galerkin-based approach for accurate non-linear normal modes through invariant manifolds. *Journal of Sound and Vibration*, 249(5):971–993, 2002. doi:10.1006/jsvi.2001.3914.

[4] R. Arquier, S. Bellizzi, R. Bouc, and B. Cochelin. Two methods for the computation of nonlinear modes of vibrating systems at large amplitudes. *Computers & Structures*, 84(24-25):1565–1576, 2006. doi:10.1016/j.compstruc.2006.01.011.

[5] M. Peeters, R. Viguié, G. Sérandour, G. Kerschen, and J.-C. Golinval. Nonlinear normal modes, part II: Toward a practical computation using numerical continuation techniques. *Mechanical Systems and Signal Processing*, 23(1):195–216, 2009. doi:10.1016/j.ymssp.2008.04.003.

[6] D. Laxalde and F. Thouverez. Complex non-linear modal analysis for mechanical systems: Application to turbomachinery bladings with friction interfaces. *Journal of Sound and Vibration*, 322(4-5):1009, 2009. doi:10.1016/j.jsv.2008.11.044.

[7] P. Alart and A. Curnier. A mixed formulation for frictional contact problems prone to newton like solution methods. *Computer Methods in Applied Mechanics and Engineering*, 92(3):353, 1991. doi:10.1016/0045-7825(91)90022-X.

[8] A.R. Mijar. Review of formulations for elastostatic frictional contact problems. *Structural and Multidisciplinary Optimization*, 20(3):167, 2000. doi:10.1007/s001580050147.

[9] N. J. Carpenter. Lagrange constraints for transient finite element surface contact. *International Journal for Numerical Methods in Engineering*, 32(1):103, 1991. doi:10.1002/nme.1620320107.

[10] T. A. Laursen and J. C. Simo. A continuum-based finite element formulation for the implicit solution of multibody, large deformation-frictional contact problems. *International Journal for Numerical Methods in Engineering*, 36(20):3451–3485, 1993. doi:10.1002/nme.1620362005.

[11] G. Pietrzak and A. Curnier. Large deformation frictional contact mechanics: continuum formulation and augmented lagrangian treatment. *Computer Methods in Applied Mechanics and Engineering*, 177 (3-4):351, 1999. doi:10.1016/S0045-7825(98)00388-0.

[12] K. C. Woo, A. A. Rodger, R. D. Neilson, and M. Wiercigroch. Application of the harmonic balance method to ground moling machines operating in periodic regimes. *Chaos, Solitons & Fractals*, 11(15): 2515–2525, 2000. doi:10.1016/S0960-0779(00)00075-8.

[13] N. Leib, S. Nacivet, F. Thouverez, and L. Jézéquel. Experimental and numerical analysis of two vibro-impacting beams. In *Proceedings of International Modal Analysis Conference*, 2007.

[14] M. F. A. Azeez and A. F. Vakakis. Numerical and experimental analysis of a continuous overhung rotor undergoing vibro-impacts. *International Journal of Non-Linear Mechanics*, 34(3):415–435, 1998. doi:10.1016/S0020-7462(98)00022-5.

[15] N. Lesaffre, J.-J. Sinou, and F. Thouverez. Stability analysis of rotating beams rubbing on an elastic circular structure. *Journal of Sound and Vibration*, 299(4-5):1005–1032, 2007. doi:10.1016/j.jsv.2006.08.027.

[16] M Legrand, C. Pierre, P. Cartraud, and J.-P. Lombard. Two-dimensional modeling of an aircraft engine structural bladed disk-casing modal interaction. *Journal of Sound and Vibration*, 319(1-2):366–391, 2009. doi:10.1016/j.jsv.2008.06.019.

[17] P. Wriggers. *Computational Contact Mechanics*. Springer Berlin Heidelberg, 2nd ed. edition, 2006. doi:10.1007/978-3-540-32609-0.

[18] M. J. D. Powell. Algorithms for nonlinear constraints that use lagrangian functions. *Mathematical Programming*, 14(1):224–248, 1978. doi:10.1007/BF01588967.

[19] J. S. Arora, A. I. Chahande, and J. K. Paeng. Multiplier methods for engineering optimization. *International Journal for Numerical Methods in Engineering*, 32(7):1485, 1991. doi:10.1002/nme.1620320706.

[20] E. Jones, T. Oliphant, P. Peterson, et al. SciPy: Open source scientific tools for Python, 2001–. URL `http://www.scipy.org/`.